Pentameric procyanidin from *Theobroma cacao* selectively inhibits growth of human breast cancer cells

Danica Ramljak,[1] Leo J. Romanczyk,[2] Linda J. Metheny-Barlow,[1] Nicole Thompson,[1] Vladimir Knezevic,[3] Mikhail Galperin,[3] Arun Ramesh,[3] and Robert B. Dickson[1]

[1]Department of Oncology, Lombardi Comprehensive Cancer Center, Georgetown University Medical Center, Washington, District of Columbia; [2]Masterfoods USA, Hackettstown, New Jersey; and [3]20/20 Gene Systems, Rockville, Maryland

Abstract

A naturally occurring, cocoa-derived pentameric procyanidin (pentamer) was previously shown to cause G_0/G_1 cell cycle arrest in human breast cancer cells by an unknown molecular mechanism. Here, we show that pentamer selectively inhibits the proliferation of human breast cancer cells (MDA MB-231, MDA MB-436, MDA MB-468, SKBR-3, and MCF-7) and benzo(*a*)pyrene-immortalized 184A1N4 and 184B5 cells. In contrast, normal human mammary epithelial cells in primary culture and spontaneously immortalized MCF-10A cells were significantly resistant. We evaluated whether this differential response to pentamer may involve depolarization of the mitochondrial membrane. Pentamer caused significant depolarization of mitochondrial membrane in MDA MB231 cells but not the more normal MCF-10A cells, whereas other normal and tumor cell lines tested gave variable results. Further investigations, using a proteomics approach with pentamer-treated MDA MB-231, revealed a specific dephosphorylation, without changes in protein expression, of several G_1-modulatory proteins: Cdc2 (at Tyr^{15}), forkhead transcription factor (at Ser^{256}, the Akt phosphorylation site) and p53 (Ser^{392}). Dephosphorylation of p53 (at Ser^{392}) by pentamer was confirmed in MDA MB-468 cells. However, both expression and phosphorylation of retinoblastoma protein were decreased after pentamer treatment. Our results show that breast cancer cells are selectively susceptible to the cytotoxic effects of pentameric procyanidin, and suggest that inhibition of cellular proliferation by this compound is associated with the site-specific dephosphorylation or down-regulation of several cell cycle regulatory proteins. [Mol Cancer Ther 2005;4(4): 537–46]

Introduction

Breast cancer is the most prevalent malignancy in women and constitutes 30% of all cancers reported in the United States (1). Current treatments in patients with early stage (localized), as well as late stage (metastatic) disease may involve surgery, followed by radiation and hormonal and/or cytotoxic chemotherapy. One of the major problems associated with drug treatments of cancer is their toxic side effect. Most of the currently used chemotherapeutic agents do not optimally discriminate between normal and tumor cells and induce cell death in all actively proliferating cells. As a result, new drug development approaches are aimed at developing compounds that specifically attack tumor cells while sparing normal cells.

Early genetic changes associated with malignancy involve genes that regulate cell cycle progression, and often these changes result in a loss of G_1 checkpoint in tumor cells due to defects in retinoblastoma protein (pRb) and p53 cell cycle pathways (2). Differences in these pathways between normal and tumor cells can be exploited in tumor cells by novel chemopreventive and chemotherapeutic approaches that selectively block the cell cycle progression.

Similarly, the mitochondrion, a cellular organelle responsible for energy production for all cellular functions, has been reported to function differently in cancer cells compared with normal cells, exhibiting a higher mitochondrial membrane potential approximately 60 mV higher than that of control cells (3). Altered mitochondrial function in tumor cells contributes to a wide array of tumor phenotypes, including higher rates of glycolysis (4), glucose transport (5), gluconeogenesis (6), and modified amino acid metabolism (7). Furthermore, various tumor cell lines exhibit differences in the number, size, and shape of their mitochondria relative to slower growing tumors and normal controls (8). Such differences between mitochondria of normal and cancer cells should enable the development of more selective and efficient cancer therapies capable of altering mitochondrial functions in cancer cells while sparing normal cells.

In a search for novel compounds that could be beneficial for cancer prevention and treatment, procyanidin and prodelphinidins (9, 10) have attracted a great deal of attention due to their wide range of biological activities. There is a growing body of evidence suggesting that these compounds act as potent antioxidants *in vitro*, *ex vivo*, and *in vivo* (11). Our interest has focused on the evaluation of several representative compounds within the procyanidin

Received 10/25/04; revised 2/4/05; accepted 2/21/05.

Grant support: Masterfoods USA.

The costs of publication of this article were defrayed in part by the payment of page charges. This article must therefore be hereby marked advertisement in accordance with 18 U.S.C. Section 1734 solely to indicate this fact.

Requests for reprints: Robert B. Dickson, Department of Oncology, The Research Building, Room W417, Lombardi Comprehensive Cancer Center, Georgetown University Medical Center, 3970 Reservoir Road, NW, Washington, DC 20057. Phone: 202-687-3770; Fax: 202-687-7505. E-mail: dicksonr@georgetown.edu

class for activity against breast cancer. Initial observations have shown that procyanidin-rich fractions prepared from the seeds of *Theobroma cacao*, which are used to prepare cocoa, inhibit *in vitro* growth of several human breast cancer cell lines (12). These studies have revealed oligomeric procyanidins, such as the pentameric procyanidin (referred to hereafter as pentamer) to be cytotoxic to breast cancer cells. The structure of the naturally occurring pentamer has been confirmed by total synthesis (12). Comparative *in vitro* studies, using the MDA MB-231 cell line, indicated growth inhibition caused by pentamer to be the result of cell cycle arrest at G_0/G_1. Moreover, a series of control experiments showed that direct actions of the compound itself caused the G_0/G_1 arrest, rather than any potential effects caused by hydrogen peroxide formed by autooxidation (12).

Collectively, these results prompted us to examine the molecular changes associated with pentamer-induced cell cycle arrest and cytotoxicity against human breast cancer cells. Our results provide evidence that pentamer selectively inhibits growth of human breast cancer cell lines, whereas normal and immortalized human mammary epithelial cells (HMEC) exhibit resistance. The mechanism seems to involve decreased phosphorylation of integral growth regulatory proteins, including p53. These results indicate the potential for pentamer to be further evaluated as a selective chemopreventive and/or chemotherapeutic of human breast cancer and possibly other human cancers.

Materials and Methods

Cell Culture

MDA MB-231, MDA MB-436, MDA MB-468, SKBR-3, and MCF-7 cell lines were obtained from the Lombardi Comprehensive Cancer Center, Tissue Culture Shared Resource and grown in complete medium containing DMEM (Life Technologies, Gaithersburg, MD) supplemented with 10% fetal bovine serum (Quality Biological, Gaithersburg, MD). Medium for MCF-7 also contained nonessential amino acids (Life Technologies).

Normal HMEC at passage 8 were purchased from Clonetics-Bio Whittaker, Inc. (Walkersville, MD) and maintained according to the supplier's instructions in mammary epithelial basal medium (Clonetics-Bio Whittaker) supplemented with 52 μg bovine pituitary extract/mL, 10 ng/mL human epidermal growth factor, 5 μg/mL insulin, and 0.5 μg/mL hydrocortisone and grown in 37°C incubators with low (0.1–0.2%) CO_2 settings. The spontaneously immortalized, nontumorigenic human mammary epithelial cell line MCF-10A and its modified counterparts MCF-10A-ErbB2/Ras (13) and MCF-10A-c-Myc (14) were maintained in F-12/DMEM supplemented with 5% horse serum (Life Technologies), 20 ng/mL epidermal growth factor (Upstate Biotechnology Incorporated, Lake Placid, NY), 10 μg/mL insulin (Biofluids, Rockville, MD), and 500 ng/mL hydrocortisone. The 184A1N4 (referred to hereafter as A1N4) and 184B5 cell lines are nontumorigenic cell lines derived from primary cultures of HMECs that were immortalized with benzo(*a*)pyrene (15) and provided by Dr. M.R. Stampfer (University of California, Berkeley, CA). A1N4 were maintained in Improved Minimum Essential Medium with 0.5% fetal bovine serum, 0.5 μg/mL hydrocortisone (Biofluids), 5 μg/mL insulin, and 10 ng/mL epidermal growth factor. 184B5 were maintained in mammary epithelial growth medium (Clonetics-Bio Whittaker).

Reagents and Antibodies

All antibodies used are listed in Table 1. Enhanced chemiluminescence detection reagent was obtained from Amersham (Arlington Heights, IL). HPLC-purified oligomeric pentameric procyanidin was provided by Masterfoods USA, Hackettstown, NJ.

Evaluation of Cellular Proliferation by Crystal Violet Assay

For breast cancer cell lines, 1×10^3 cells per well were seeded in 96-well dishes (Corning Costar, Cambridge, MA). Primary cultures of HMECs, A1N4 and 184B5 cells were evaluated at two different cell densities (1×10^3 and 2×10^3 per well). After 24 hours, cells in triplicate wells were treated with pentamer at a concentration of 100 μg/mL or equal volume of DMSO vehicle. At indicated time points up to 10 days, cells were stained with crystal violet as described previously (16) and the absorbance at 550 nm was analyzed on an Ultramark Microplate Imaging System (Bio-Rad, Philadelphia, PA). Two to three independent experiments were done in triplicate. The unpaired Student's *t* test was used to determine significance of differences.

Mitochondrial Membrane Potential

Mitochondrial membrane potential was evaluated using the ApoAlert mitochondrial membrane sensor kit (Clontech, Inc., Palo Alto, CA). Cells were first grown to 60% to 70% confluence in 25 cm^2 dishes. The next day, the medium was replaced with fresh medium containing pentamer (25 or 100 μg/mL), DMSO or medium only. At the indicated time, floating and adherent cells were combined, and 1×10^6 cells analyzed according to the manufacturer's instructions. Samples were analyzed at the Lombardi Comprehensive Cancer Center, Core Flow Cytometry Shared Resource Facility.

Multilayered Dot Blot of Liquid Samples in Multiwell Plates

Multilayered dot blot is a recently developed method for screening liquid protein samples in a high-throughput manner using multiwell plates (17–19) and was conducted in collaboration with 20/20 Gene Systems, Inc., (Rockville, MD) as previously described (18). Briefly, MDA MB-231 cells were treated with vehicle or 100 μg/mL pentamer for 48 or 72 hours, and cell pellets lysed in multilayered dot blot lysis buffer (20/20 Gene Systems). Protein concentrations were determined by using a bicinchoninic acid protein assay kit (Pierce, Rockford, IL). Ten and 20 μg of each protein sample were loaded in duplicate into a Bio-Dot Microfiltration Apparatus (Bio-Rad) and transferred through a five-membrane stack as recommended by the manufacturer (20/20 Gene Systems). After

transfer, membranes were biotinylated in 1 mg/mL EZ-Link Sulfo-NHS-Biotin solution (Pierce), then incubated overnight at 4°C with 45 primary antibodies (listed in Table 1). After washing, the membranes were incubated with a mixture of FluoroLink Cy 5-labeled streptavidin (Amersham) and fluorescein-labeled secondary anti-mouse or anti-rabbit antibody (Molecular Probes, Eugene, OR).

Table 1. Antibodies used in multilayered dot blot and immunoblotting

Protein/antibody	Dilution	Source	Secondary antibodies	Application
PARP (H-250)	1:1,000	Santa Cruz	rabbit	IB
α-Tubulin	1:3,000	Neomarkers	mouse	IB
GAPDH	1:500	Chemicon	rabbit	IB
Cleaved caspase 3 (Asp^{175})	1:500	Cell Signaling	rabbit	MLDot
Cleaved caspase 7 (Asp^{198})	1:500	Cell Signaling	rabbit	MLDot
Cleaved PARP	1:500	Cell Signaling	rabbit	MLDot
Cleaved caspase 9 (Asp^{330})	1:500	Cell Signaling	rabbit	MLDot
p38-Mitogen-activated protein kinase-P	1:500	Cell Signaling	rabbit	MLDot
p44/42-Mitogen-activated protein kinase-P	1:500	Cell Signaling	rabbit	MLDot
Stress-activated protein kinase/c-*Jun*-NH_2-kinase-P	1:500	Cell Signaling	rabbit	MLDot + IB
pRb MIX-pRb (Ser^{795}) + pRb ($Ser^{807/811}$)	1:1,000 each	Cell Signaling	rabbit	MLDot + IB
pRb	1:1,000	Santa Cruz	rabbit	IB
CHK2-P	1:500	Cell Signaling	rabbit	MLDot
CHK1-P	1:500	Cell Signaling	rabbit	MLDot
Cdc2-P (Tyr^{15})	1:500	Cell Signaling	rabbit	MLDot + IB
Cdc2	1:000	Cell Signaling	rabbit	IB
p53-P	1:500	Cell Signaling	rabbit	MLDot
p53	1:1,000	Cell Signaling	rabbit	IB
Stat-P (MIX)-Stat 3-Tyr^{701} + Stat 3 Ser^{727}	1:1,000 each	Cell Signaling	rabbit	MLDot
Stat 3-P Tyr^{705}	1:500	Cell Signaling	rabbit	MLDot
Stat 1-P Tyr^{701}	1:500	Cell Signaling	rabbit	MLDot
Stat 6-P Tyr^{641}	1:500	Cell Signaling	rabbit	MLDot
Stat 5-P (Tyr^{694})	1:500	Cell Signaling	rabbit	MLDot + IB
PTEN-P (Ser^{380})	1:500	Cell Signaling	rabbit	MLDot
AKT-P (mix of Ser^{473}/Thr^{308})	1:1,000 each	Cell Signaling	rabbit	MLDot
AKT-total	1:500	Cell Signaling	rabbit	MLDot
PDK1-P (Ser^{241})	1:500	Cell Signaling	rabbit	MLDot
GSK3-β-P(Ser^{9})	1:500	Cell Signaling	rabbit	MLDot
FKHR-P (Ser^{256})	1:500	Cell Signaling	rabbit	MLDot + IB
FKHR	1:1,000	Cell Signaling	rabbit	IB
PKD/PKC-($Ser^{744/748}$)	1:500	Cell Signaling	rabbit	MLDot
PKC/PKC-M (Ser^{916})	1:500	Cell Signaling	rabbit	MLDot
PKC-δ (Ser^{643})	1:500	Cell Signaling	rabbit	MLDot + IB
PKC-α/β II-P ($Thr^{638/641}$)	1:500	Cell Signaling	rabbit	MLDot
PKC-PAN-P (βII/Ser^{660})	1:500	Cell Signaling	rabbit	MLDot
PKC-ξ/λ-P ($Thr^{410/403}$)	1:500	Cell Signaling	rabbit	MLDot
PKC-θ-P (Thr^{538})	1:500	Cell Signaling	rabbit	MLDot +IB
PKC-δ-P (Thr^{505})	1:500	Cell Signaling	rabbit	MLDot
P53-P Cocktail 1 (Ser^{6}, Ser^{9}, and Ser^{20})	1:1,000 each	Cell Signaling	rabbit	MLDot + IB
P53-P (Ser^{15})	1:500	Cell Signaling	rabbit	IB
P53-P Cocktail 2 (Ser^{37}, Ser^{46}, and Ser^{392})	1:1,000 each	Cell Signaling	rabbit	MLDot + IB
Epidermal growth factor receptor	1:500		mouse	MLDot
p44/42-Mitogen-activated protein kinase-total	1:500	Cell Signaling	rabbit	MLDot
Epidermal growth factor receptor-P (Tyr^{1173})	1:500	Upstate Biotechnology	mouse	MLDot
Bcl-xL	1:500	Santa Cruz	rabbit	MLDot
mTOR-P (Ser^{2448})	1:500	Cell Signaling	rabbit	MLDot
Bcl-2	1:500	Neomarkers	mouse	MLDot
Mouse IgG	1:2,000	Molecular Probes	mouse	MLDot + IB
Rabbit IgG	1:2,000	Molecular Probes	rabbit	MLDot + IB

Abbreviations: MLDot, multilayered dot blot; IB, immunoblotting.

Confirmation of Multilayered Dot Blot Results by Immunoblotting

Protein pellets from vehicle or pentamer-treated MDA MB-231, MDA MB-468, and MCF-7 cells were lysed in PBS with 1% SDS and sonicated, then protein concentrations analyzed as above. Ten micrograms of each protein sample was separated on 4% to 20% gradient gels (Bio-Rad) and transferred to polyvinylidene difluoride (PVDF) membranes (Bio-Rad) or P-FILM membrane (stacks of 10 membranes, 20/20 Gene Systems) according to manufacturer's instructions. Membranes were incubated overnight at 4°C in primary antibodies (Table 1), followed by horseradish peroxidase-conjugated secondary antibody, developed with Enhanced Chemiluminescence Plus reagent (Amersham) and signals visualized on BIOMAX MR film (Kodak, Rochester, NY). glyceraldehyde-3-phosphate dehydrogenase (GAPDH) was visualized by secondary antibody conjugated to alkaline phosphatase DuoLux substrate (Vector Laboratories, Burlingame, CA). PVDF membranes were stripped using a protocol provided by Cell Signaling (Beverly, MA) and reprobed as indicated.

High-Resolution Profiling of p53 and pRb

The protein samples used for PVDF membranes (described previously) were used in these experiments. Ten micrograms of each protein sample from vehicle or pentamer (100 μg/mL)–treated cells were separated by PAGE on 4% to 20% gradient gels (Bio-Rad) and transferred onto a stack of 10 multilayered dot blot membranes as above; the antibodies used are listed in Table 1. The secondary antibody used in all cases was anti-rabbit at 1:2,000 dilution (Amersham). Image analysis for both proteins was done with Kodak one-dimensional image analysis software. Background-corrected intensity values were normalized for loading by using GAPDH intensities. Numerical analysis was done in Excel.

Results

Breast Cancer Cells Exhibit Higher Sensitivity to Pentamer-Induced Growth Inhibition Compared with Normal and Immortalized Mammary Epithelial Cells

Previous studies examined the effects of procyanidins derived from cocoa on the cell cycle of human breast cancer cells (12). The results indicated that the pentamer, but not the lower oligomeric compounds, caused G_0/G_1 cell cycle arrest. The pentameric form was therefore subjected to further study in order to determine whether its inhibitory action was selective for tumor cells and to gain insight into the mechanism(s) responsible for this activity.

We first used the crystal violet assay to evaluate the effects of pentamer on the growth of a panel of human breast cancer cell lines (MDA MB-231, MDA MB-436, MD MB-468, and SKBR3) compared with human immortalized (MCF-10A, 184B5, and A1N4) and normal primary HMECs. All experiments were done using 100 μg/mL of pentamer, a dose shown to be effective in growth inhibition, as previously described (12). The data showed that the growth of MDA MB-231 and MDA MB-436 was significantly inhibited (5.1-fold and 4.6-fold, respectively) compared with DMSO-treated controls (Fig. 1A and B; Table 2). SKBR-3 cells were growth-inhibited 5.5-fold and MDA MB-468 cells were 4.2-fold more growth-inhibited in comparison to DMSO-treated controls (Table 2).

In order to test the selectivity of pentamer for cancer cells, the sensitivity of spontaneously immortalized MCF-10A cells and normal mortal HMECs was tested as described above. Whereas MCF-10 cells were completely resistant to the growth-inhibitory effects of pentamer (Fig. 1C), slight inhibition of normal primary HMEC growth was observed (about 1.45-fold, Fig. 1D). HMECs were 2- to 4-fold less sensitive to the growth-inhibitory effects of pentamer compared with cancer cells (Fig. 1A, B, and D; Table 2).

However, when benzo(*a*)pyrene immortalized 184B5 cells were tested, they exhibited greater sensitivity (2.4-fold, Table 2) to pentamer than HMECs or MCF-10A. Interestingly, benzo(*a*)pyrene-immortalized A1N4 cell line exhibited very high sensitivity to pentamer (6.8-fold growth inhibition) compared with controls (Table 2). The level of sensitivity of A1N4 cells was similar to that of human breast cancer cells. The results of pentamer treatment–mediated growth inhibitory effects at day 10 post-treatment on all cell lines tested are summarized in Table 2.

Resistance to Pentamer of MCF-10A and Mortal HMECs Is Independent of Their Proliferation Rate

In order to determine whether pentamer resistance of MCF-10A cells and normal HMECs was due to the slow proliferation rate of these cells, we next evaluated the effects of pentamer on the growth of parental MCF-10A cells (population doubling time, 31.4 hours) compared with highly proliferating MCF-10A-c-Myc (MCF-10A cells transduced with c-Myc) with a population doubling time of 20.4 hours (14) and MCF-10A-ErbB2/Ras (with a 4-fold more rapid doubling time compared with parental MCF-10A cells; ref. 13) using crystal violet assay as above. We observed that, similar to parental MCF-10A cells, both MCF-10A-c-Myc and MCF-10A-ErbB2/Ras were resistant to pentamer-induced growth inhibition (data not shown). Based on these results, we conclude that the resistance of MCF-10A to pentamer does not result from slower proliferation rate.

Growth-Inhibitory Effects of Pentamer Are Independent of p53 and Estrogen Receptor Status

The MDA MB-231, MDA MB-436, MDA MB-468, and SKBR-3 breast cancer cell lines tested (Table 2) all lack estrogen receptor expression and have mutant p53. In order to test whether p53 mutations or estrogen receptor status influence response to pentamer, we analyzed the growth of pentamer-treated estrogen receptor–positive MCF-7 breast cancer cells bearing wild-type p53. As shown in Table 2, pentamer treatment caused significant growth inhibition of MCF-7 as well, indicating that growth-inhibitory effects of pentamer against human breast cancer cells are not determined by the status of estrogen receptor or p53.

Pentamer-Induced Depolarization of Mitochondrial Membrane Potential of Breast Cancer Cell Lines

Based on the differential sensitivities of breast cancer cells compared with MCF-10A or normal HMECs in response to pentamer, we hypothesized that differences in mitochondrial function between breast cancer cells and their normal or immortalized mammary epithelial cell counterparts might be involved. We first tested the pentamer for its effects on mitochondrial membrane potential of MDA MB231 tumor cells compared with the MCF10A cell line. Preliminary studies indicated that 6-hour treatment achieved maximal mitochondrial membrane potential loss and was used for subsequent studies. MDA MB-231 cells exhibited a high degree of mitochondrial membrane depolarization (52%) in response to pentamer, compared with 5% to 10% in DMSO-treated controls (data not shown). By contrast, pentamer treatment caused depolarization of the mitochondrial membrane in only 19% of the MCF-10A cells, where the DMSO background was only 9% (data not shown). Analysis of other tumor cell lines and the immortalized A1N4 cell line were more variable; although in MDA MB-436, MDA MB-468, and A1N4 cells pentamer also caused significant depolarization of the mitochondrial membrane (5.7-, 5.0-, and 3.2-fold, respectively), neither SKBR-3 nor MCF-7 tumor cells showed consistently significant depolarization in response to pentamer (data not shown). As a result, we are unable to draw a conclusion about the effect of pentamer on mitochondrial membrane potential at this time.

Pentamer Targets Cell Cycle and Apoptosis Proteins in Breast Cancer Cells

To identify the molecular targets that could provide insight into the mode of inhibitory action of pentamer, we further investigated protein samples of DMSO and pentamer-treated MDA MB-231 human breast cancer cells by proteomic multilayered dot blot analysis (18). The proteomics approach provides information on both expression and activity of proteins. MDA MB-231 cells were selected because they are highly susceptible to the growth-inhibitory effects of the compound (Fig. 1A). The proteins selected as potential targets of pentamer for detailed screenings were those commonly involved in the control of cellular

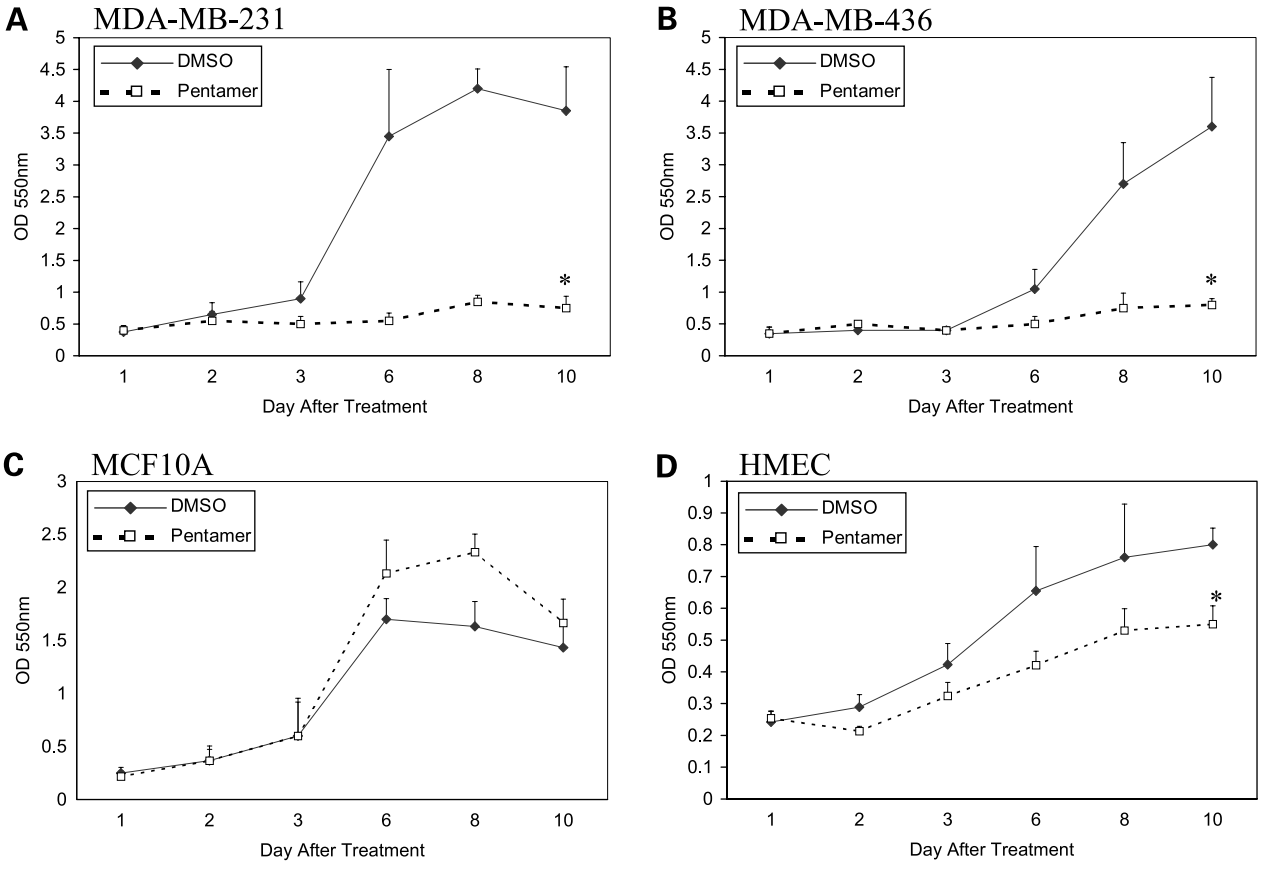

Figure 1. Pentamer selectively inhibits the growth of human breast cancer cells compared with spontaneously immortalized and normal mortal HMECs. Human breast cancer MDA MB-231 (**A**) and MDA MB-436 (**B**), nontransformed spontaneously immortalized MCF-10A (**C**), and normal mortal HMEC (**D**) cells were grown in triplicate in 96-well plates and treated with 100 μg/mL of pentamer (*hashed line*) or DMSO vehicle (*solid line*) for up to 10 d as described in Materials and Methods. Samples were collected at the indicated days post-pentamer treatment and analyzed by crystal violet assay as described. The data presented are an average from triplicate wells from two to three independent experiments. Bars, SD; *, statistical significance compared with DMSO treated controls ($P < 0.0001$).

Table 2. Effects of pentamer on growth inhibition of breast cancer cell lines compared with mammary epithelial cells

Cell culture	Transformation status	Mean absorbance (DMSO control)	Mean absorbance (pentamer)
HMEC	Normal primary	0.80 ± 0.05	0.55 ± 0.06*
MCF-10A	Spontaneously immortalized	1.43 ± 0.25	1.70 ± 0.22 †
184.B5	Benzo(*a*)pyrene immortalized	0.79 ± 0.06	0.33 ± 0.01*
184.A1N4	Benzo(*a*)pyrene immortalized	1.50 ± 0.21	0.22 ± 0.04*
MCF7	Breast cancer	3.22 ± 0.95	1.07 ± 0.70*
MDA MB-231	Breast cancer	3.85 ± 0.70	0.75 ± 0.19*
MDA MB-436	Breast cancer	3.65 ± 0.77	0.79 ± 0.12*
MDA MB-468	Breast cancer	1.96 ± 0.82	0.47 ± 0.15*
SKBR-3	Breast cancer	2.20 ± 0.78	0.40 ± 0.20*

NOTE: Breast cancer, normal, or immortalized HMEC treated 10 days with pentamer or vehicle were analyzed by crystal violet assay and absorbance was measured at 550 nm. Data are presented as mean absorbance from two to three independent experiments done in triplicate ± SD.
*$P < 0.001$, Student's t test.
†Not statistically significant ($P = 0.0795$).

growth, proliferation, survival, and apoptosis (Table 1). A total of 46 different antibodies were used in this screening with emphasis placed on the relative phosphorylation status of potentially active proteins. The results indicated that the phosphorylation status for eight proteins [Cdc2, forkhead transcription factor (FKHR), p53, protein kinase C (PKC)-δ, PKC-θ-, pRb, stress-activated protein kinase/c-*Jun*-NH_2-kinase, and Stat 5] had been affected by pentamer, whereas total protein levels were unaffected (Fig. 2A and data not shown). We further noted that phosphorylation status for five out of these eight proteins was affected by pentamer within 48 hours (Cdc2, PKCδ, pRb, stress-activated protein kinase/c-*Jun*-NH_2-kinase, Stat5); decrease ranged from 22% to 36% (data not shown). Phosphorylation was significantly decreased in all eight proteins after 72 hours of pentamer treatment, ranging from 26% (stress-activated protein kinase/c-*Jun*-NH_2-kinase) to 63% in the case of FKHR (data not shown). Ward hierarchical clustering analysis showed clear segregation between control and treated groups based on the behavior of proteins examined.

Using immunoblotting, we confirmed the multilayered dot blot results on phosphorylated forms of Cdc2 (Tyr^{15}), FKHR (Ser^{256}), p53 (Ser^{37}, Ser^{46}, and Ser^{392}) and pRb (Ser^{795} and $Ser^{807/811}$; Fig. 2B). Total protein expression was not affected by pentamer as evidenced by multilayered dot blot analysis (Fig. 2A), and Western analysis confirmed equal expression of total Cdc2, p53, and FKHR (Fig. 2C). However, levels of both total and phosphorylated pRb were decreased by pentamer (Fig. 2C). Equal loading was confirmed by GAPDH expression (Fig. 2B and C). Using current experimental immunoblotting conditions and PVDF membranes, we could not confirm the multilayered dot blot results for PKC-δ, PKC-θ, stress-activated protein kinase/c-*Jun*-NH_2-kinase, and Stat5.

Pentamer Decreases Phosphorylation of p53 (Ser^{392}) and pRb (Ser^{780}, Ser^{795}, and $Ser^{807/811}$) in Human Breast Cancer Cells

Both p53 and pRb contain a number of phosphorylation sites, and each site determines specific protein function. Because pentamer elicits a G_0/G_1 cell cycle growth arrest (12) and both p53 and pRb play crucial roles in controlling this phase of the cell cycle, we did high-resolution functional profiling of these two proteins in MDA MB-231 cells treated with 100 μg/mL of pentamer or DMSO vehicle using P-FILM technology (20/20 Gene Systems).

The levels of endogenous p53 expression in MDA MB-231 cells were slightly decreased in pentamer-treated samples after only 48 hours (Fig. 3A). Densitometry suggests that this decrease was not significant (data not shown). Profiling the serine residues of p53 revealed only slight decreases in phosphorylation of Ser^{15} residue and Ser^{46} at 48 hours post-treatment (Fig. 3A and B), whereas significant dephosphorylation of p53 Ser^{392} residue was detected in response to pentamer at both 48 and 72 hours post-treatment (Fig. 3A). Additional confirmation of the p53 results was obtained by traditional immunoblotting (Fig. 3B). Phosphorylation of the Ser^{20} residue was decreased at 48 hours, but was not affected in samples treated with pentamer for 72 hours (Fig. 3A).

To further evaluate p53 dephosphorylation on Ser^{392} by pentamer, we next analyzed p53 status in the MDA MB-468 (mutated p53) and the MCF-7 (wild-type p53) cell lines following treatment with pentamer. Similar to MDA MB-231 cells, expression of p53 in MDA MB-468 was not significantly affected by pentamer treatment (Fig. 3B). However, the percentage of p53 phosphorylated at Ser^{392} was decreased in both MDA MB-231 (53% compared with untreated controls) and MD MB-468 cells (33% compared with untreated controls; Fig. 3B), whereas neither Ser^{15} or Ser^{46} was significantly affected in MDA MB-468 cells (Fig. 3B). Under similar experimental conditions, we could not detect any signal for endogenous wild-type p53 or phosphorylated p53 in MCF-7 cells (Fig. 3B). This result was expected because it has been shown that endogenous levels of wild-type p53 are not easily detected by immunoblotting, whereas mutated p53 detection is more readily demonstrable due to its overexpression (20). The equality of loading in all cell lines tested was confirmed by equal expression of GAPDH protein levels (Fig. 3A and B).

In order to perform profiling of pRb phosphorylation in response to pentamer, the samples were analyzed for expression of total pRb and for the phosphorylation status of pRb at Ser^{780}, Ser^{795}, and $Ser^{807/811}$ in MDA MB-231 cells. We found that pentamer treatment caused a decrease in protein expression of endogenous pRb, possibly resulting in the decrease of phosphorylation on all tested residues (Fig. 3C). The expression of GAPDH protein was not changed, indicating equal loading of samples.

Discussion

The goal of the present study was to test the selectivity of oligomeric pentameric procyanidin from cocoa (pentamer) against a panel of human breast cancer cells and to examine the molecular mechanism(s) by which it causes G_0/G_1 cell cycle arrest in these cells (12). This is, to our knowledge, the first demonstration that pentamer selectively inhibits growth of human breast cancer cell lines independent of their p53 or estrogen receptor status, whereas normal HMECs and nontransformed, immortalized MCF-10A cells are highly resistant. The resistance of normal HMECs to pentamer's cytotoxicity relative to highly sensitive human breast cancer cells is significant because it could serve as a basis for *in vivo* evaluation of pentamer as a potential chemopreventive and chemotherapeutic agent in both animal models and human disease.

We first evaluated whether pentamer's inhibitory effects involve depolarization of the mitochondrial membrane. The MDA MB-231 cells were highly sensitive, whereas the mitochondria of MCF-10A cells were only slightly affected by pentamer. Similarly, the induction of mitochondrial depolarization by structurally different, small molecular weight polyphenolics have recently been reported (21). However, whereas both the SKBR-3 and MCF-7 tumor cell lines were highly growth-inhibited by pentamer (Table 2), neither consistently showed significant depolarization of the mitochondrial membrane. It has previously been shown that pentamer can exert two distinct effects on cancer cells, growth arrest and cytotoxicity (12), which may contribute to the net growth inhibition observed in all tumor cell lines in our study. The mitochondrial effects caused by pentamer

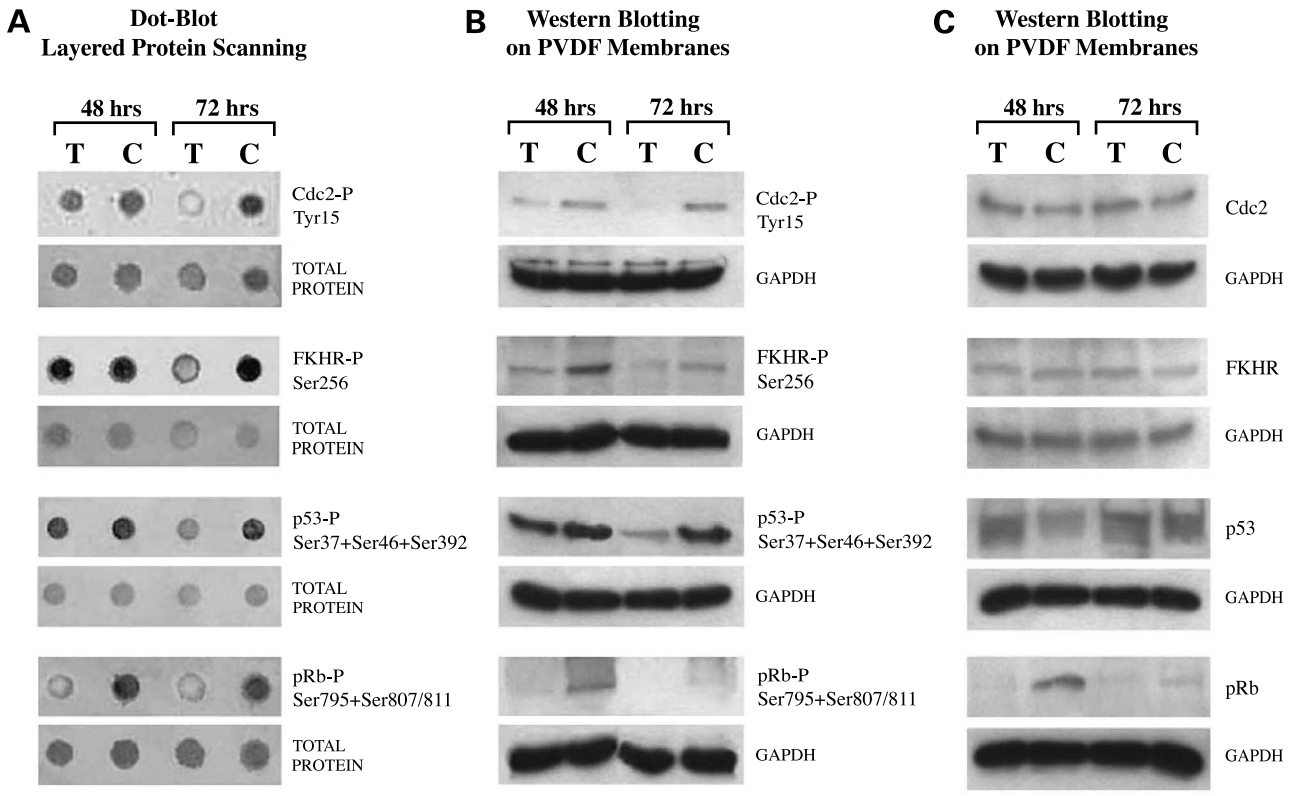

Figure 2. Multilayered dot blot multiwell plate and immunoblotting analysis (PVDF membrane) of pentamer-treated human breast cancer cells. **A,** MDA MB-231 cells were treated with 100 μg/mL of pentamer (*T*) for 48 and 72 h and control cells were treated with DMSO (*C*). Twenty micrograms of protein lysates were first loaded into the wells of 96 multilayered dot blot multiwell plates, and later transferred through the stack of five membranes. After transfer, all of the membranes were biotinylated, probed with antibodies listed in Table 1, and visualized with fluorescein-labeled secondary antimouse or antirabbit antibody and total protein expression determined with FluoroLink Cy 5-labeled streptavidin. **B,** 10 μg of the same samples from (**A**) were analyzed by traditional immunoblotting for the indicated phosphorylated proteins using PVDF membrane. Protein samples were visualized by Typhoon scanner. **C,** membranes from (**B**) were stripped and reprobed with antibodies detecting Cdc2, FKHR p53, and pRb independent of their phosphorylation status. To test for equality of loading, blots were reprobed with GAPDH. The results are representative of two independent immunoblotting analyses using the same protein samples.

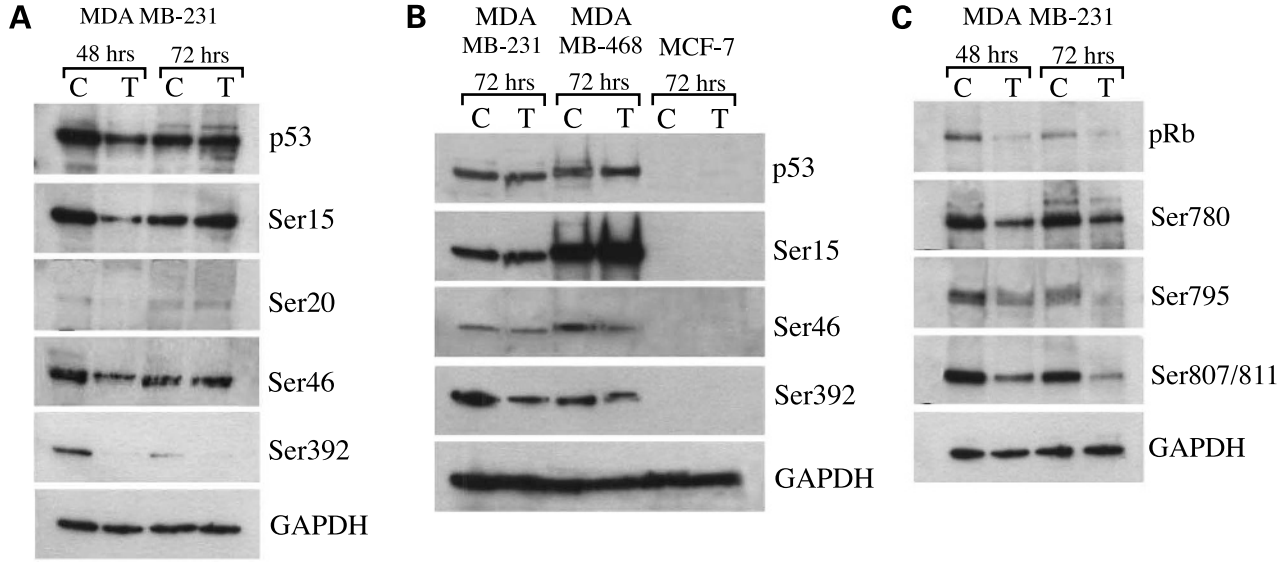

Figure 3. High-resolution profiling of p53 and pRb in human breast cancer cells treated with pentamer. **A,** MDA MB-231 cells treated with pentamer for 48 and 72 h and corresponding DMSO-treated controls were analyzed by immunoblotting analysis. A total of six membranes were generated from the same gel and each membrane was probed with different specific antibody-recognizing endogenous p53 and four different phosphorylation residues of p53 that were suspected to be affected by pentamer after initial screening using multilayered dot blot. **B,** separate immunoblotting experiments were done using protein lysates prepared in parallel from MDA MB-231, MDA MB-468, and MCF-7 cells treated with pentamer and DMSO for 72 h. To test for equality of loading, blots were probed with GAPDH. The data are representative of two independent immunoblotting analyses using the same protein samples. **C,** the same protein lysates of pentamer- and DMSO-treated controls of MDA MB-231cells analyzed above were used in immunoblotting for pRb. A total of five membranes were generated from the same protein gel and membranes were probed with antibodies detecting endogenous pRb and phosphorylation sites at Ser^{780}, Ser^{795}, and $Ser^{807/811}$. To test for equality, loading blots were probed with GAPDH.

could be expected to trigger either growth arrest or apoptotic or nonapoptotic cell death processes. Indeed, recent studies using the novel mitochondriotoxic small molecule F16 suggested that compounds causing mitochondrial depolarization inhibited tumor growth of breast cancer cells by G_1 cell cycle arrest (22), apoptosis (23), or necrosis (23), depending on the genetic background of the cell. The lack of sensitivity to mitochondrial membrane depolarization in response to pentamer in certain tumor cell lines may therefore reflect the involvement of mitochondrial membrane potential loss in only one of the two inhibitory activities associated with pentamer, growth arrest or cell death. Future studies will be required to precisely address the role of mitochondrial membrane depolarization in the inhibitory action of pentamer.

Similar to breast cancer cells, benzo(*a*)pyrene-immortalized A1N4 were highly sensitive to pentamer-mediated growth inhibition, whereas 184B5 cells exhibited a lesser degree of sensitivity (Table 2). The underlying cellular basis for pentamer sensitivity of these two lines is unknown. Our results in 184B5 cells are consistent with previously reported sensitivity to growth inhibition of these cells to tea polyphenol (−) epigallocatechin gallate and soy isoflavone genistein (24).

We next sought to identify the molecular events that contribute to the inhibitory effects of pentamer on breast cancer cells. We therefore selected the highly sensitive MDA MB-231 cells for further molecular analysis. Initial multilayered dot blot screen using pentamer-treated MDA MB-231 cells revealed that pentamer decreases phosphorylation of eight proteins involved in control of cell cycle and apoptosis (Fig. 2A and data not shown), although immunoblotting confirmed these results for only Cdc2, p53, pRb, and FKHR (Fig. 2B). Cdc2 can promote both cell cycle progression and apoptosis (25), and its phosphorylation at Tyr^{15} is inhibitory for these activities (26); furthermore, ErbB2 phosphorylation of Cdc2 at Tyr^{15} causes resistance to taxol-induced apoptosis (26). The pentamer-induced dephosphorylation of Cdc2 at Tyr^{15} is therefore of particular interest for its potential to facilitate apoptosis. Similarly, pentamer caused a decrease in the Akt/protein kinase B–dependent phosphorylation site of FKHR (Ser^{256}; Fig. 2A and B). This is of importance, because Akt phosphorylation of FKHR Ser^{256} is critical to the ability of growth factors to suppress FKHR-dependent transcription, thereby preventing FKHR from inducing cell cycle arrest and apoptosis through transcriptional regulation of p27 (kip1; ref. 27) and FKHR-controlled Fas ligand expression (28–30).

We further showed that in MDA MB-231 and MDA MB-468 cells, pentamer specifically dephosphorylates p53 at Ser^{392} without affecting the other serine residues we evaluated (Ser^6, Ser^9, Ser^{15}, Ser^{20}, Ser^{46}, and Ser^{37}). The phosphorylation of Ser^{392}, in particular, activates specific DNA binding functions by stabilizing p53 tetramer formation (31), and several stress stimuli are reported to

phosphorylate Ser^{392} (Ser^{389} in mouse; ref. 32). Furthermore, increased phosphorylation of p53 at Ser^{392} is frequent in human tumors (33, 34) and correlates with increased aggressiveness (33), indicating that pentamer-mediated dephosphorylation of Ser^{392} may be of importance.

Detailed evaluation of pRb status and its phosphorylation in MDA MB-231 revealed that pentamer decreased the protein expression of pRb itself, a likely explanation for observed decreased phosphorylation of this protein at Ser^{780}, Ser^{795}, and $Ser^{807/811}$, all residues critically involved in G_1-S transition (35, 36). Similar to pentamer, transforming growth factor-β and retinoic acid have been reported to cause G_1 cell cycle arrest by causing dephosphorylation of pRb at Ser^{780}, Ser^{795}, and $Ser^{807/811}$ (37, 38). A more detailed time course of the kinetics of pRb decreased phosphorylation relative to its overall downregulation requires further study.

In summary, we provide novel evidence that pentamer selectively inhibits proliferation of human breast cancer cell lines. We have further identified a number of critical proteins known to be activated (phosphorylated) in cancer cells whose phosphorylation status has been normalized in the presence of pentamer. Future studies will be aimed at elucidating the precise role of these proteins in pentamer's inhibitory action, particularly p53, which has recently been shown to translocate to mitochondria (39). Of particular interest will be investigations of possible connections between pentamer's effects on cell cycle and its effects on mitochondria; it should be noted that the mitochondriotoxic molecule F16 is also capable of eliciting growth arrest and cell death that is associated with dephosphorylation of specific growth regulatory proteins (22). Furthermore, it will be important to establish the relevance of observed *in vitro* anticancer effects of pentamer in *in vivo* preclinical breast cancer models. Such studies will be helpful for the evaluation of pentamer as an effective chemopreventive and chemotherapeutic agent against human breast cancer.

Acknowledgments

We thank Dr. Karen Creswell of the Lombardi Comprehensive Cancer Center at Georgetown University for performing flow cytometry analyses, technical personnel (Shuangju Lu, Lisa S. Cahill, Feng Zhu, and Victoria A. North) of the Lombardi Comprehensive Cancer Center Tissue Culture Shared Resources (which is partially supported by NIH Grant 3P30-CA-51008), as well as Doug Gallo for technical input. We also thank Drs. James Rae and Marc Lippman (Department of Internal Medicine, University of Michigan, Ann Arbor, MI) for helpful advice early in the course of this study.

References

1. Funkhouser WK, Kaiser-Rogers K. Review: significance of, and optimal screening for, HER2 gene amplification and protein overexpression in breast carcinoma. Ann Clin Lab Sci 2001;31:349 – 58.

2. Lomazzi M, Moroni MC, Jensen MR, Frittoli E, Helin K. Suppression of the p53- or pRB-mediated G_1 checkpoint is required for E2F-induced S-phase entry. Nat Genet 2002;31:190 – 4.

3. Modica-Napolitano JS, Aprille JR. Basis for selective cytotoxicity of rhodamine 123. Cancer Res 1987;47:4361 – 5.

4. Pedersen PS, Frederiksen O, Holstein-Rathlou NH, Larsen PL, Qvortrup K. Ion transport in epithelial spheroids derived from human airway cells. Am J Physiol 1999;276:L75 – 80.

5. Dang CV, Lewis BC, Dolde C, Dang G, Shim H. Oncogenes in tumor metabolism, tumorigenesis, and apoptosis. J Bioenerg Biomembr 1997;29:345 – 54.

6. Lundholm K, Edstrom S, Karlberg I, Ekman L, Schersten T. Glucose turnover, gluconeogenesis from glycerol, and estimation of net glucose cycling in cancer patients. Cancer 1982;50:1142 – 50.

7. Souba WW. Glutamine and cancer. Ann Surg 1993;218:715 – 28.

8. Carafoli E. Mitochondria and disease. Mol Aspects Med 1980;3: 295 – 429.

9. Harborne JB. The flavenoids. Advances in research since 1986. Chapman & Hall; 1994.

10. Hemingway RW. Structural variations in proanthocyanidins and their derivatives. In: Hemingway RW, Karchesy JJ, editors. Chemistry and significance of condensed tannins. Plenum Publishing; 1989. p. 83 – 107.

11. Huan MT, Ho CT, Lee CY. Pheonolic compounds in foods and their effects on health. II. Antioxidants and cancer prevention. ACS Symposium Series 507. Washington, DC: American Chemical Society; 1992.

12. Kozikowski AP, Tuckmantel W, Bottcher G, Romanczyk LJ Jr. Studies in polyphenol chemistry and bioactivity. 4.(1) Synthesis of trimeric, tetrameric, pentameric, and higher oligomeric epicatechin-derived procyanidins having all-4,8-interflavan connectivity and their inhibition of cancer cell growth through cell cycle arrest. J Org Chem 2003;68:1641 – 58.

13. Ciardiello F, Gottardis M, Basolo F, et al. Additive effects of c-erbB-2, c-Ha-ras, and transforming growth factor- genes on *in vitro* transformation of human mammary epithelial cells. Mol Carcinog 1992;6:43 – 52.

14. Sheen JH, Dickson RB. Overexpression of c-Myc alters G(1)/S arrest following ionizing radiation. Mol Cell Biol 2002;22:1819 – 33.

15. Stampfer MR, Bartley JC. Induction of transformation and continuous cell lines from normal human mammary epithelial cells after exposure to benzo[*a*]pyrene. Proc Natl Acad Sci U S A 1985;82: 2394 – 8.

16. Shaik MS, Chatterjee A, Singh M. Effects of monensin liposomes on the cytotoxicity, apoptosis and expression of multidrug resistance genes in doxorubicin-resistant human breast tumour (MCF-7/dox) cell-line. J Pharm Pharmacol 2004;56:899 – 907.

17. Englert CR, Baibakov GV, Emmert-Buck MR. Layered expression scanning: rapid molecular profiling of tumor samples. Cancer Res 2000;60:1526 – 30.

18. Galperin MM, Traicoff JL, Ramesh A, et al. Multimembrane dot-blotting: a cost-effective tool for proteome analysis. BioTechniques 2004;36:1046 – 51.

19. Traicoff JL, Galperin MM, Ramesh A, et al. Profiling the expression of mitogen-induced T-cell proteins by using multi-membrane dot-blotting. Biochem Biophys Res Commun 2004;323:355 – 60.

20. DiCioccio RA, Werness BA, Peng R, Allen HJ, Piver MS. Correlation of TP53 mutations and p53 expression in ovarian tumors. Cancer Genet Cytogenet 1998;105:93 – 102.

21. Galati G, Teng S, Moridani MY, Chan TS, O'Brien PJ. Cancer chemoprevention and apoptosis mechanisms induced by dietary polyphenolics. Drug Metabol Drug Interact 2000;17:311 – 49.

22. Fantin VR, Berardi MJ, Scorrano L, Korsmeyer SJ, Leder P. A novel mitochondriotoxic small molecule that selectively inhibits tumor cell growth. Cancer Cell 2002;2:29 – 42.

23. Fantin VR, Leder P. F16, a mitochondriotoxic compound, triggers apoptosis or necrosis depending on the genetic background of the target carcinoma cell. Cancer Res 2004;64:329 – 36.

24. Katdare M, Osborne MP, Telang NT. Inhibition of aberrant proliferation and induction of apoptosis in pre-neoplastic human mammary epithelial cells by natural phytochemicals. Oncol Rep 1998; 5:311 – 5.

25. Konishi Y, Lehtinen M, Donovan N, Bonni A. Cdc2 phosphorylation of BAD links the cell cycle to the cell death machinery. Mol Cell 2002;9:1005 – 16.

26. Tan M, Jing T, Lan KH, et al. Phosphorylation on tyrosine-15 of p34(Cdc2) by ErbB2 inhibits p34(Cdc2) activation and is involved in resistance to taxol-induced apoptosis. Mol Cell 2002; 9:993 – 1004.

27. Martinez-Gac L, Alvarez B, Garcia Z, et al. Phosphoinositide 3-kinase and Forkhead, a switch for cell division. Biochem Soc Trans 2004;32:360 – 1.

28. Jackson JG, Kreisberg JI, Koterba AP, Yee D, Brattain MG. Phosphorylation and nuclear exclusion of the forkhead transcription factor FKHR after epidermal growth factor treatment inhuman breast cancer cells. Oncogene 2000;19:4574 – 81.

29. Nakamura N, Ramaswamy S, Vazquez F, et al. Forkhead transcription factors are critical effectors of cell death and cell cycle arrest downstream of PTEN. Mol Cell Biol 2000;20:8969 – 82.

30. Dijkers PF, Medema RH, Pals C, et al. Forkhead transcription factor FKHR-L1 modulates cytokine-dependent transcriptional regulation of p27(KIP1). Mol Cell Biol 2000;20:9138 – 48.

31. Keller DM, Zeng X, Wang Y, et al. A DNA damage-induced p53 serine 392 kinase complex contains CK2, hSpt16, and SSRP1. Mol Cell 2001;7:283 – 92.

32. Fiscella M, Zambrano N, Ullrich SJ, et al. The carboxy-terminal serine 392 phosphorylation site of human p53 is not required for wild-type activities. Oncogene 1994;9:3249 – 57.

33. Minamoto T, Buschmann T, Habelhah H, et al. Distinct pattern of p53 phosphorylation in human tumors. Oncogene 2001;20:3341 – 7.

34. Furihata M, Kurabayashl A, Matsumoto M, et al. Frequent phosphorylation at serine 392 in overexpressed p53 protein due to missense mutation in carcinoma of the urinary tract. J Pathol 2002; 197:82 – 8.

35. Kitagawa M, Higashi H, Jung HK, et al. The consensus motif for phosphorylation by cyclin D1-Cdk4 is different from that for phosphorylation by cyclin A/E-Cdk2. EMBO J 1996;15:7060 – 9.

36. Panigone S, Debernardi S, Taya Y, et al. pRb and Cdk regulation by *N*-(4-hydroxyphenyl)retinamide. Oncogene 2000;19:4035 – 41.

37. Hu X, Cress WD, Zhong Q, Zuckerman KS. Transforming growth factor inhibits the phosphorylation of pRB at multiple serine/threonine sites and differentially regulates the formation of pRB family-E2F complexes in human myeloid leukemia cells. Biochem Biophys Res Commun 2000;276:930 – 9.

38. Dimberg A, Bahram F, Karlberg I, et al. Retinoic acid-induced cell cycle arrest of human myeloid cell lines is associated with sequential down-regulation of c-Myc and cyclin E and posttranscriptional up-regulation of p27(Kip1). Blood 2002;99:2199 – 206.

39. Dumont P, Leu JI, Della Pietra AC 3rd, George DL, Murphy M. The codon 72 polymorphic variants of p53 have markedly different apoptotic potential. Nat Genet 2003;33:357 – 65.